Selection of machining condition on surface integrity of additive and conventional Inconel 718

S. Periane, Arnaud Duchosal, S. Vaudreuil, H. Chibane, Antoine Morandeau, M. Anthony Xavior, R. Leroy

Available online at www.sciencedirect.com

ScienceDirect

Procedia CIRP 00 (2019) 000–000

www.elsevier.com/locate/procedia

5th CIRP CSI 2020

Selection of machining condition on surface integrity of additive and conventional Inconel 718

S. Periane[a*], A. Duchosal[a], S.Vaudreuil[b], H.Chibane[c], A.Morandeau[d], M. Anthony Xavior[e], R. Leroy[a]

[a]*Univ. Tours, Univ. Orléans, INSA CVL, LaMé, 7 Avenue Marcel Dassault, Tours 37200, France,*
[b]*Euromed University of Fes, Morocco*
[c] *INSA Strasbourg, CSIP, 24 Boulevard de la Victoire,67084 Strasbourg Cedex, France*
[d]*Advanced Assisted Manufacturing Solutions (AAMS), Bâtiment CEROC, Rue Henri Garih, 37230 Fondettes, France*
[e]*Manufacturing Department, School of Mechanical Engineering, VIT University, Vellore - 632014, India*

* Corresponding author. Tel.: +33 (0) 761034269 ; *E-mail address:* natarajan.sasidharanperiane@etu.univ-tours.fr

Abstract

Inconel 718 is a nickel-based superalloy used in steam turbines, jet engines, etc., where it is subjected to high thermomechanical loads. Inconel 718 is the most preferred alloy in the above applications due to its excellent resistance to fatigue and creep. Inconel 718 is mainly strengthened by the precipitates which were formed during the heat treatment process by the combination of elements like Nb, Ti, and Al along with the base element Ni. Selective Laser Melting (SLM) is one of the most used additive manufacturing processes to manufacture components with high dimensional accuracy in a flexible manner with less material usage. The samples fabricated by SLM were subjected to two heat treatments: Hot Isostatic Pressing (HIP) to improve the density followed by the Aeronautic Heat Treatment (AHT) in order to improve the material properties. The heat-treated SLM samples have the same mechanical properties of the conventional Inconel 718 fabricated by the Cast and Wrought (C&W). The Central Composite face-centered Design (CCD) was used for the Design of Experiments (DOE) in which three different cutting speeds (v_c) and feed rates (f_z) were considered whereas the depth of cut (a_p) is kept constant. Machining experiments were conducted under dry, Minimum Quantity Lubrication (MQL) and emulsion (Wet) conditions on both the cast and wrought (C&W) Inconel 718 and additive fabricated SLM Inconel 718. The optimum cutting condition for C&W and SLM Inconel 718 samples was determined based on three criteria: minimum specific cutting energy (Wc), minimum tool wear (Vb) and minimum surface roughness (Ra). From the overall results, it is being inferred that the SLM Inconel 718 produced better results compared to C&W Inconel 718.

Keywords: SLM; MQL; DOE

1. Introduction

Nickel-based superalloy like Inconel 718 was widely used in the aero-engines particularly to fabricate turbine disks [1]. The 3D parts can be realized in the SLM technique with less material usage. The parts were fabricated in an inert Nitrogen (Ni) or Argon (Ar) environment [2]. The laser power used is sufficient enough to melt the powder to a required depth in order to form a good metallurgical bonding during solidification. The laser beam rapidly melts and solidifies the powder, which leads to thermal variations (to expand and contract at different rates) [3,4] generating high-density dislocations [5]. The thermal variation leads to anisotropy in the material, which can be reduced by subjecting the as-built samples to heat treatments like HIP and AHT. The HIP (Hot Isostatic Pressing) is very essential for parts made of powder to improve its material properties and to reduce the porosity in order to maximize the working life of the parts [6]. Followed

by AHT, the purpose of this heat treatment is to dissolve the segregation of the particles and to facilitate the population of the strengthening precipitates [7]. Generally Inconel 718 material has poor machinability [8–10] due to its low thermal conductive property [11,12]. During machining, it tends to form a build-up edge [13]. The self-hardening mechanism leads to the higher cutting force due to which the tool life is very less [14]. To increase the tool life to even a few minutes while machining Inconel 718 is a great challenge. An enormous amount of heat is produced while machining Inconel 718, of which a large portion of the produced heat transfers to the tool compared to the material and the chip. The heat accumulated at the cutting zone is ≈1000°C results in the diffusion of carbide particles which weakens the bonding between the carbides and binder. The above mechanism leads to the plastic deformation of the cutting edge which is the main reason for the low tool life [15]. In addition to it, the work hardening behavior of the material tends to induce notch wear at the depth of cut which results in poor surface roughness [16]. Therefore, it is essential to induce good surface integrity on the workpiece in order to satisfy the fatigue properties especially for aerospace materials like Inconel 718 [17]. In order to reach properties such as minimum surface roughness on additive parts finish machining is essential. In the machinability study, Design of Experiments (DOE) was performed by changing the cutting speed and feed rate under dry, MQL and wet conditions, where the depth of cut is kept constant. The MQL choice is based on the results from the work of A.Duchosal et al [18] whose result shows that MQL machining provides better surface roughness.

To the author's best of knowledge only a few works on milling of Inconel 718 especially additive samples has been reported. The objective of this work is to determine the optimum machining conditions based on the DOE results which provide good machinability domains that fulfill the economic criteria.

2. Methodology

2.1. Sample fabrication and post-processing

Inconel 718 Gas Atomized (GA) powder supplied by Multistation enterprise, France was used for the fabrication of samples. The most common and economical way of producing powder is Gas Atomized (GA) method. The chemical composition of the powder is shown in Table 1 which consists of elements and its corresponding weight percentage.

Table 1: Chemical composition of the Inconel 718 powder.

El.	Al	Co	Cr	Mn	Mo	Nb+Ta	Ni	Ti
wt%	0.2	1	21	0.3	3.3	5.5	55	1.15

The powder particle characterization such as video granulometry analysis was done using Horiba Camsizer X2 at UEMF University, Fes, Morocco. The powder particle size distribution analysis was done in the Camsizer instrument by which the powder particles of nominal size 40 – 90 µm were used for fabrication, the SEM image of the powder particles is shown in Fig. 1(a).

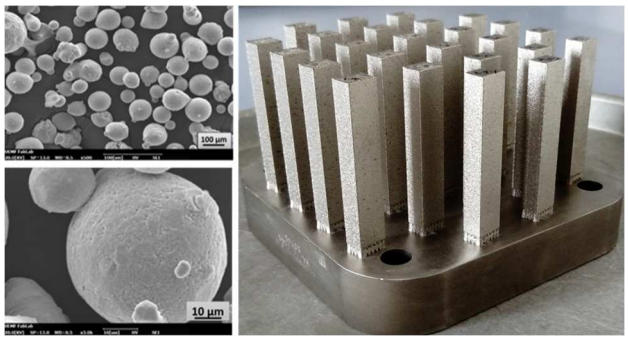

(a) (b)

Fig. 1: (a) GA powder particles and (b) vertically oriented samples.

The samples were modeled using Materialise Magics Builds software and then fabricated using SLM 125 HL machine. The samples were fabricated at a distance of 12 mm as shown in Fig. 1 (b). The process parameters used are 200 W laser power and the scanning speed of 800 mm/s. The hatch distance was maintained at 120 µm and the layer thickness of 50 µm for a minimum scanning time of 12 seconds. The fabrication was done in a controlled nitrogen atmosphere using a stripes pattern.

The grain formation mechanism is not proper in the additive fabrication, only the fused powder layers (melt pool) are visible along with the pores in the as-built microstructure. The Hot Isostatic Pressing (HIP) was done to diffuse the melt pool boundaries, in which the temperature was first increased to the target temperature of 1160°C at a pressure of 102 MPa maintained for 3hrs in order to obtain 99.99% dense sample. The HIP alone was not sufficient, so AHT was done after HIP process where the samples were maintained at 720°C/8 hours followed by cooling in the furnace for 1.5 hours until 650°C/8 hours followed by air cooling up to room temperature. The change is microstructure was realised by EBSD analysis (step size of 1µm) using the Carl Zeiss Supra 40 [19].

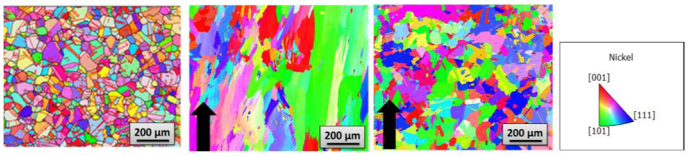

(a) (b) (c)

Fig. 2: Microstructure of (a) C&W (b) As-built and (c) HIP+AHT (arrow mark shows the build direction).

The Cast &Wrought alloy has a random texture and no preferred orientation with a grain size of 15-25 µm and δ phase fraction of 1.5 to 2% as shown in Fig. 2 (a). The major difference between the as-built and the heat-treated microstructure is the complete dissolution of the columnar arc-shaped melt pool layers [20] and the diffusion of pores as shown in the Fig. 2 (b). The material gets a very fine and homogenous grain structure after undergoing (HIP+AHT) heat treatment process. High content of γ and γ'' phases and low

content of δ phase can be obtained by the heat treatment process as shown in Fig. 2 (c). The top face of the vertically oriented sample is 8% harder compared to the bottom face is due to the presence of the brittle laves phase.

2.2. Design of experiments

The design of experiments (DOE) was performed with 11 tests each with different cutting conditions like varying speed and feed rates in dry, MQL and wet conditions. The application of central composite face-centered design (CCD) is a standard, reliable, and popular design that can be efficiently used to assess the interaction between variables. CCD contains an embedded factorial or fractional factorial design with points that are augmented with a group of the axial point that allows the estimation of curvature. Although rotatability is a desirable property of CCD, in case of difficulty to extend the axial points beyond the experimental zone defined by the upper and lower limits of each factor a face-centered design can be used in order to save the material. The machining protocol is shown in Table 2.

Table 2: Machining protocol.

V_c (m/min)	f_z (m/min)	a_p (mm)	Cutting environment		
20	0.05				
30	0.10	0.5	Dry	MQL	Wet
40	0.15				

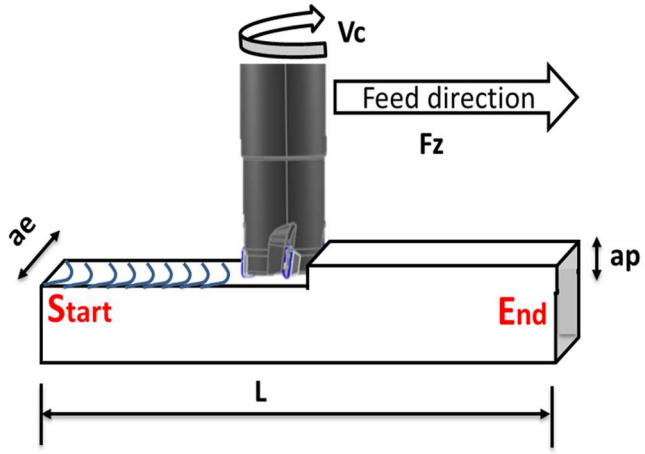

Fig. 3: Schematic diagram of the machining protocol.

The force at the start and end was taken into consideration and the roughness (Ra) was measured for each machining condition along the length of the sample, L= 60 mm and width a_e = 9 mm a shown in Fig. 3. In this study, the central composite face-centered design (CCD) and response surface methodology were applied to design the experiments and to evaluate the interactive effects of the three most important variables.

The DOE 's face centered composite design was adopted to model the response of the specific cutting energy for C&W and SLM produced sample in dry, MQL and wet conditions. The effects were studied with the response to the specific cutting energy (Wc) which is given in Eq. 1.

$$Specific\ cutting\ energy = \frac{\text{Power}(W)}{\text{Material removal rate}(cm\text{^}3/min)} \quad (1)$$

The DOE was performed with the set of experiments shown in Table 3 where the middle cutting condition was repeated three times (3R). The outcome was the resultant cutting force measurement for these varying cutting conditions. From the cutting force value, the objective is to find the optimum machining condition suitable for Inconel 718 in dry, MQL and wet conditions in terms of specific cutting energy (Wc). The design of experiments Modde software was used for plotting the data.

Table 3: Design of experiments.

Experiment number	V_c (m/min)	f_z (mm/tooth)
N1	20	0.05
N2	20	0.15
N3	20	0.1
N4	40	0.05
N5	40	0.15
N6	40	0.1
N7	30	0.05
N8	30	0.15
N9	30	0.1
N10	30	0.1
N11	30	0.1

2.3. Machining conditions

The machining tests were performed on the 5 axes Hermle C40U CNC machine. The oil mist was created by an external generator (Lubrilean Digital Super) developed by SKF.

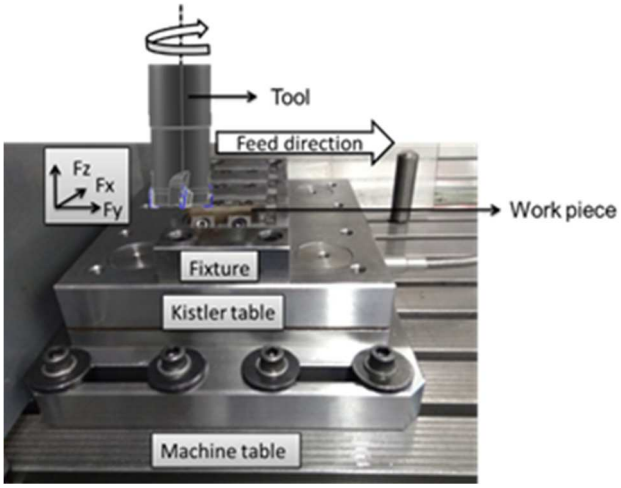

Fig. 4: Machining set-up with the KISTLER dynamometer table (type 9255B).

A computer is connected to the generator to change the mist settings by maintaining a pressure of 2 bar at a flow rate of 70 ml/hr. The MQL oil used was Vascomill MMS SE1 special oil based on synthetic esters from Blaser. The emulsion for the wet condition is from IGOL USINOV 2475 used at pressure of 30

bar, 7% concentration. The samples were mounted on a specially designed fixture which was fixed on to the Kistler 9255B type dynamometric table. The cutting forces were measured in three orthogonal directions Fx, Fy and Fz, which corresponds to cutting direction, feed direction and the axial direction as shown in Fig. 4.

Table 4: Insert details.

Insert reference: 390R-70204E-ML1040	
Lead angle	90 deg
Coating	PVD (Ti, Al) N_2
Corner radius (reinforced edge)	0.4 mm
Edge radius ER	27µm ± 3µm

The tool used in this study: R390-020A20-07M with the internal cooling channel for emulsion and MQL, along with the insert mentioned in Table 4 which was recommended and provided by SANDVIK CORMANT. The cutting-edge radius (ER) of the inserts was controlled using the GFM MikroCAD® equipment. According to the ISO 3685 standard on tool life, no further machining was done when the insert attains average flank wear (Vb) = 0.3mm. The tool wear measurement was controlled using the Stream Essentials image analysis software.

3. Results and discussions

3.1. Wc, Roughness and Vb in Dry machining

The DOE in dry machining was performed to have a reference for the MQL and emulsion (wet) conditions. As well as to better understand the cutting mechanisms.

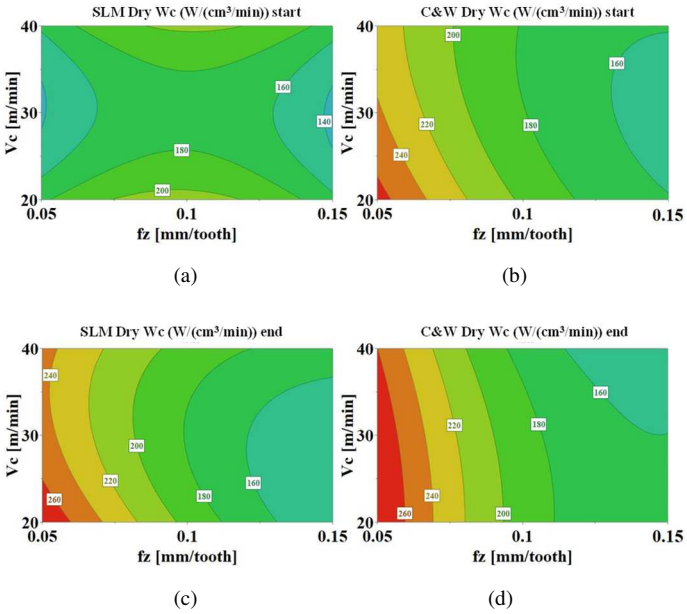

Fig. 5: Variation of Wc in (a) dry condition start for SLM (R^2=1.0) (b) start C&W (R^2=1.0) (c) end SLM (R^2=0.91) and (d) end C&W (R^2=0.98).

In Fig. 5, the contour plot of Wc was represented for different cutting speeds (V_c) and feed rates (f_z) in dry machining for the cast and wrought (C&W) and SLM Inconel 718 for the depth of cut (a_p) 0.5 mm. The specific cutting energy (Wc) decreases with an increase in the feed rate.

At the start of the machining shown in Fig. 5 (a,b), the SLM sample consumed nearly 23% less cutting energy compared to the C&W alloy. Whereas at the end of machining shown in Fig. 5 (c,d) the energy consumption is similar for both the C&W and SLM samples. The result shows that even though the C&W and the SLM sample have nearly the same mechanical properties but different microstructure has benefitted the SLM sample in consuming less specific cutting energy (Wc) than the C&W sample. In the zone of tool functionality according to AFNOR (E66-520) norm, the most dominant cutting process is shearing whereas outside this zone only rubbing (more friction and less machining) is taking over shearing.

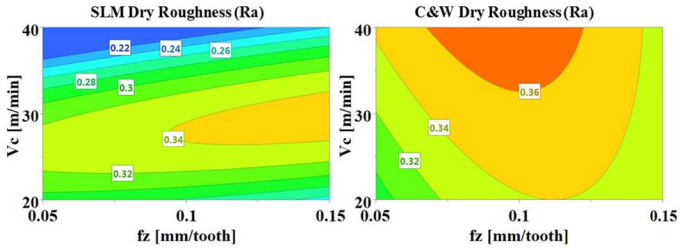

Fig. 6: Variation of average Ra between start and end for (a) SLM (R^2=0.98) and (b) C&W (R^2=0.91) in dry condition.

Fig. 6 shows the variation of roughness values Ra for C&W and SLM Inconel 718 alloy. In general, for the C&W variation of roughness is very small of ±0.2µm compared to the SLM sample. In Fig. 6 (a) the Ra increases linearly in the range of ≈0.02 µm as the cutting speed increases.

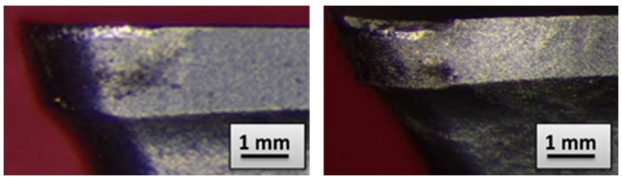

Fig. 7: Flank wear (Vb) on dry machining of (a) SLM and (b) C&W.

At the same time, the flank wear (Vb) of the tool is 0.09 mm for the SLM sample, whereas it linearly increased up to 0.25 mm on the machining of the C&W sample (Fig. 7). This indicates again the microstructural variation has more influence on the machining process.

The optimum cutting conditions for the C&W sample is in the range of V_c 35-40 m/min and f_z 0.13-0.15mm/tooth. For the SLM sample, the V_c 35-40 m/min and f_z 0.05-0.15 mm/ tooth obtained based on the minimum Wc and minimum Ra.

3.2. Wc, Roughness and Vb in MQL assisted machining

The use of MQL oil for machining SLM samples (Fig. 8) has reduced the energy consumption by nearly 15% compared

to the dry condition. The energy consumption for the SLM is 15- 22% higher on the start with reference to the end of the machining process. This indicates that MQL assistance has reduced the cutting force for the SLM (Fig. 8 (a,c)). The C&W sample consumed nearly 46% more specific cutting energy (Wc) at low speed and high feed at the end of the machining as shown in Fig. 8 (d) compared to the start (Fig. 8 (b)).

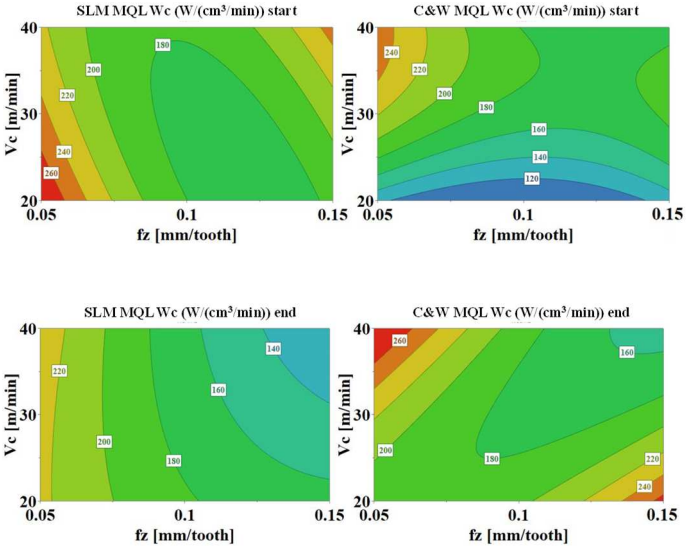

(a) (b)

(c) (d)

Fig. 8: Variation of Wc in MQL condition for (a) start SLM (R^2=0.91) (b) start C&W (R^2=0.98) (c) end SLM (R^2=0.92) and (d) end C&W (R^2=0.96).

Minimum surface roughness (Ra) is obtained for the lowest feed (f_z) and cutting speed (v_c) value as shown in Fig. 9. From Fig. 9 (a,b) the variation in the roughness value shows that nearly two times better roughness can be obtained at V_c 20 m/min and f_z 0.05 mm/ tooth in using MQL compared to the dry condition.

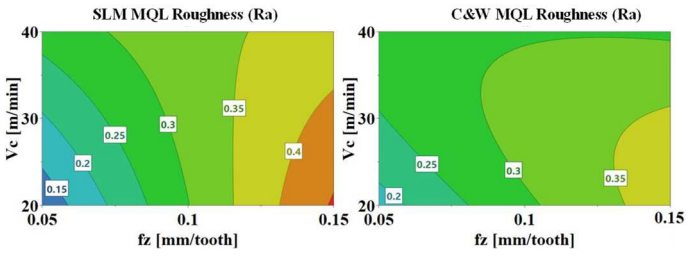

(a) (b)

Fig. 9: Variation of Ra for (a) SLM (R^2=0.96) and (b) C&W (R^2=0.92) in MQL condition.

This phenomenon of variation in the roughness could be due to the activation of the MQL oil at a low feed rate. Whereas at higher feed rate the MQL oil gets carbonized before reaching the cutting zone. The Vb obtained after machining SLM sample is 0.06 mm and C&W is 0.17 mm as shown in Fig. 10 (a,b).

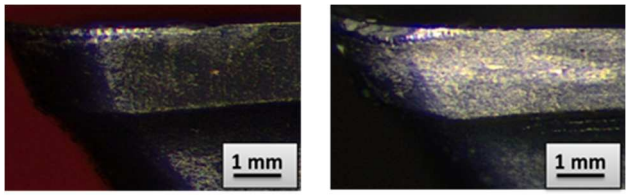

(a) (b)

Fig. 10: Flank wear (Vb) on MQL machining of (a) SLM and (b) C&W.

The optimum cutting condition for the SLM sample the V_c 20-40 m/min and f_z 0.075-0.085 mm/tooth and for the C&W sample is V_c 25 – 40 m/min and the f_z 0.1-0.15 mm/tooth.

3.3. Wc, roughness and Vb in wet machining

The SLM samples when machined using emulsion shown in Fig. 11 has reduced the energy consumption of about 38 % compared to the dry condition and 27% less compared to MQL.

The energy consumption of the C&W samples both at the start and the end (Fig. 11 (b,d)) is about 220-260 W/(cm^3/min) for the V_c 28-40 m/min and feed of 0.05-0.06 mm/tooth. In the case of the SLM sample as shown in Fig. 11 (a,c) the energy consumption is between 160-220 W/(cm^3/min) for the same range of cutting conditions.

This reduced energy consumption for the SLM sample is due to the less insert wear rate compared to the C&W machining. The wear rate while machining C&W samples is dependent on the machining environment. Whereas while machining SLM samples the wear rate is independent of the machining environment.

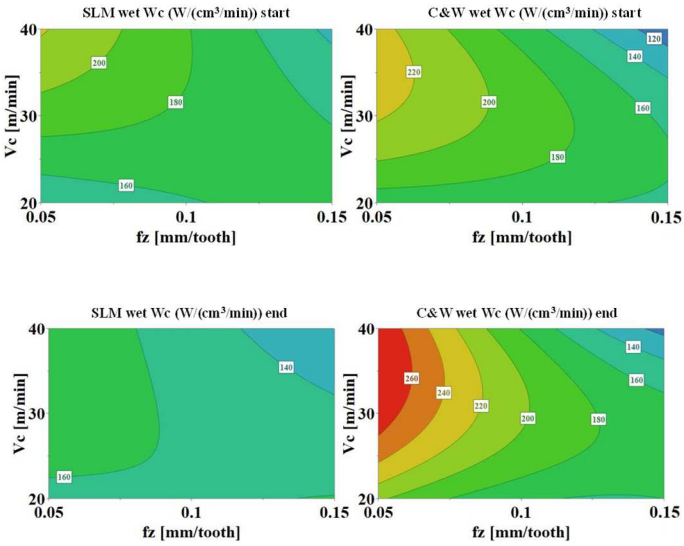

(a) (b)

(c) (d)

Fig. 11: Variation of Wc in wet condition for (a) start SLM (R^2=0.93) (b) start C&W (R^2=0.98) (c) end SLM (R^2=0.94) and (d) end C&W (R^2=0.92).

The surface roughness (Ra) is better for the SLM sample under the emulsion environment at the higher cutting conditions compared to the roughness of the C&W sample

(Fig. 12).

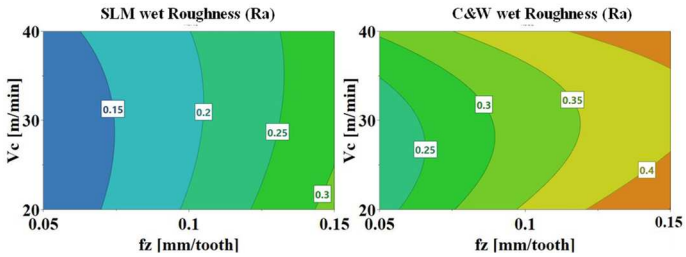

Fig. 12: Variation of Ra for (a) SLM (R^2=0.92) and (b) C&W (R^2=0.94) in emulsion condition.

The roughness variation (Ra) linearly increases at a rate of 0.10 µm for the corresponding increase in the feed rate. The Vb obtained after machining SLM sample is 0.04 mm and C&W is 0.09 mm as shown in Fig. 13.

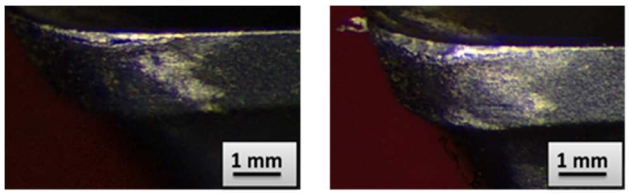

Fig. 13: Flank wear (Vb) on wet machining of (a) SLM and (b) C&W.

The optimum cutting condition for the C&W sample is V_c 20 m/min and the f_z 0.05-0.075 mm/tooth based on less energy consumption and better surface roughness. For the SLM sample, the cutting conditions of V_c 20-30 m/min and f_z 0.05-0.15 mm/tooth fulfills the criteria of minimum energy consumption and minimum roughness. This means one can machine with higher productivity in SLM fabricated Inconel 718 under wet condition.

4. Conclusions

In this research work, face milling was performed to evaluate the machinability aspects of Cast & Wrought and SLM Inconel 718. Two consecutive heat treatments (HIP+AHT) were performed on the SLM samples in order to attain the same tensile and hardness properties as that of the Cast and Wrought sample. Further, machining was performed on both the samples in dry, MQL and wet conditions. The specific cutting energy (Wc), the roughness (Ra) and the flank wear (Vb) of the tool were measured after machining both C&W and SLM samples in order to determine the optimum machining conditions. Based on the results obtained the specific cutting energy (Wc) for the dry and the MQL is similar but the zone of functionality for the MQL condition is nearly two times larger compared to the dry condition. The emulsion results are better than dry and the MQL results in terms of less energy consumption and less surface modification. The high tool wear on machining the C&W alloy compared to the SLM sample could be due to the presence of δ phase in the C&W alloy.

In general, it is concluded that using emulsion gives good machining results for Inconel 718, particularly the SLM sample has good machinability compared to the C&W Inconel 718 sample irrespective of the machining conditions.

Acknowledgments

The authors would like to thank, Dr. Jonathan CORMIER from Institut Pprime/ISAE-ENSMA, Poitiers, France and Dr. Alexis NICOLAY from CEMEF, Ecole des Mines de Paris, France for EBSD analysis and the cutting tool research centre operators (CEROC, France) for their machining support.

References

[1] S. Ford, M. Despeisse, Additive manufacturing and sustainability: an exploratory study of the advantages and challenges, J. Clean. Prod. 137 (2016) 1573–1587. doi:10.1016/j.jclepro.2016.04.150.

[2] M. Schmidt, M. Merklein, D. Bourell, D. Dimitrov, T. Hausotte, K. Wegener, L. Overmeyer, F. Vollertsen, G.N. Levy, Laser based additive manufacturing in industry and academia, CIRP Ann. 66 (2017) 561–583. doi:10.1016/j.cirp.2017.05.011.

[3] M. Xia, D. Gu, G. Yu, D. Dai, H. Chen, Q. Shi, Porosity evolution and its thermodynamic mechanism of randomly packed powder-bed during selective laser melting of Inconel 718 alloy, Int. J. Mach. Tools Manuf. 116 (2017) 96–106. doi:10.1016/j.ijmachtools.2017.01.005.

[4] L.E. Murr, Metallurgy of additive manufacturing: Examples from electron beam melting, Addit. Manuf. 5 (2015) 40–53. doi:10.1016/j.addma.2014.12.002.

[5] Q. Jia, D. Gu, Selective laser melting additive manufacturing of TiC/Inconel 718 bulk-form nanocomposites: Densification, microstructure, and performance, J. Mater. Res. 29 (2014) 1960–1969. doi:10.1557/jmr.2014.130.

[6] M.E. Aydinöz, F. Brenne, M. Schaper, C. Schaak, W. Tillmann, J. Nellesen, T. Niendorf, On the microstructural and mechanical properties of post-treated additively manufactured Inconel 718 superalloy under quasi-static and cyclic loading, Mater. Sci. Eng. A. 669 (2016) 246–258. doi:10.1016/j.msea.2016.05.089.

[7] T. Alam, M. Chaturvedi, S.P. Ringer, J.M. Cairney, Precipitation and clustering in the early stages of ageing in Inconel 718, Mater. Sci. Eng. A. (2010). doi:10.1016/j.msea.2010.08.053.

[8] R.L. Peng, J. Zhou, S. Johansson, A. Billenius, V. Bushlya, J.-E. Stahl, Surface Integrity and the Influence of Tool Wear in High Speed Machining of Inconel 718, 13th Int. Conf. Fract. (2013) 1–10.

http://www.gruppofrattura.it/ocs/index.php/ICF/icf13/paper/viewFile/11483/10862.

[9] D. Umbrello, Investigation of surface integrity in dry machining of Inconel 718, (2013) 2183–2190. doi:10.1007/s00170-013-5198-0.

[10] G.R. Thellaputta, P.S. Chandra, C.S.P. Rao, Machinability of Nickel Based Superalloys: A Review, Mater. Today Proc. 4 (2017) 3712–3721. doi:10.1016/j.matpr.2017.02.266.

[11] W. Li, Y.B. Guo, M.E. Barkey, J.B. Jordon, Effect tool wear during end milling on the surface integrity and fatigue life of inconel 718, Procedia CIRP. 14 (2014) 546–551. doi:10.1016/j.procir.2014.03.056.

[12] A. Shokrani, V. Dhokia, S.T. Newman, Hybrid Cooling and Lubricating Technology for CNC Milling of Inconel 718 Nickel Alloy, Procedia Manuf. 11 (2017) 625–632. doi:10.1016/j.promfg.2017.07.160.

[13] M. Anthony Xavior, M. Manohar, P.M. Madhukar, P. Jeyapandiarajan, Experimental investigation of work hardening, residual stress and microstructure during machining Inconel 718, J. Mech. Sci. Technol. 31 (2017) 4789–4794. doi:10.1007/s12206-017-0926-2.

[14] P. Jeyapandiarajan, M.A. Xavior, Experimental Investigations on the Machinability of Inconel 718 Under Different Cutting Conditions, 38 (2017) 295–304.

[15] R.S. Pawade, S.S. Joshi, P.K. Brahmankar, Effect of machining parameters and cutting edge geometry on surface integrity of high-speed turned Inconel 718, Int. J. Mach. Tools Manuf. 48 (2008) 15–28. doi:10.1016/j.ijmachtools.2007.08.004.

[16] S. Zhang, J.F. Li, Y.W. Wang, Tool life and cutting forces in end milling Inconel 718 under dry and minimum quantity cooling lubrication cutting conditions, 32 (2012). doi:10.1016/j.jclepro.2012.03.014.

[17] S. Kumar, D. Singh, N.S. Kalsi, Experimental Investigations of Surface Roughness of Inconel 718 under different Machining Conditions, Mater. Today Proc. 4 (2017) 1179–1185. doi:10.1016/j.matpr.2017.01.135.

[18] A. Duchosal, R. Leroy, L. Vecellio, C. Louste, N. Ranganathan, An experimental investigation on oil mist characterization used in MQL milling process, Int. J. Adv. Manuf. Technol. 66 (2013) 1003–1014. doi:10.1007/s00170-012-4384-9.

[19] A. Nicolaÿ, J.M. Franchet, J. Cormier, H. Mansour, M. de Graef, A. Seret, N. Bozzolo, Discrimination of dynamically and post-dynamically recrystallized grains based on EBSD data: application to Inconel 718, J. Microsc. 273 (2019) 135–147. doi:10.1111/jmi.12769.

[20] B. Farber, K.A. Small, C. Allen, R.J. Causton, A. Nichols, J. Simbolick, M.L. Taheri, Correlation of mechanical properties to microstructure in Metal Laser Sintering Inconel 718, Mater. Sci. Eng. A. 712 (2018) 539–547. doi:10.1016/j.msea.2017.11.125.